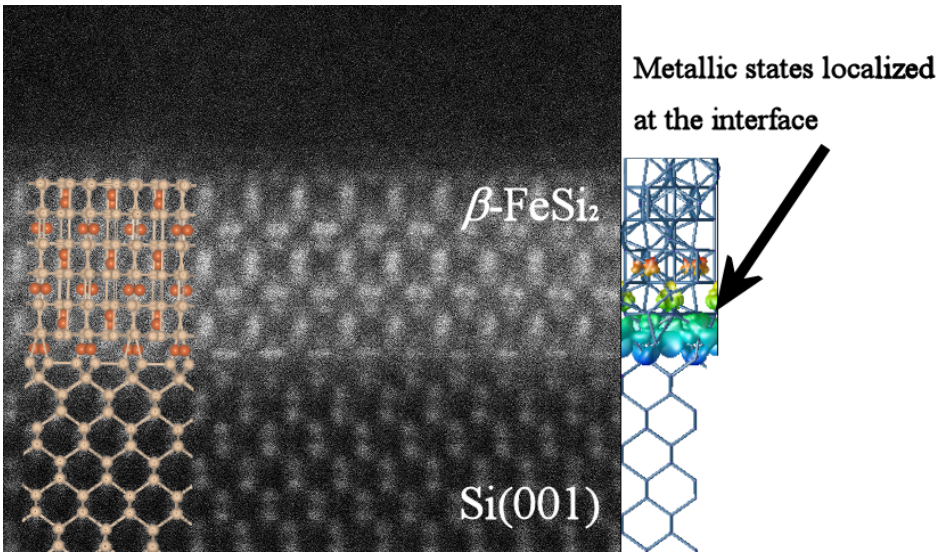
Graphical Abstract

Atomic and electronic structures of the β-$FeSi_2$/Si(001) interface

Keisuke Sagisaka, Kazutaka Mitsuishi



Highlights

Atomic and electronic structures of the β-$FeSi_2$/Si(001) interface

Keisuke Sagisaka, Kazutaka Mitsuishi

- The atomistic interface structure between β-$FeSi_2$/Si(001) substrate has been determined via STEM observations and DFT calculations.
- A high quality single crystalline β-$FeSi_2$ film was epitaxialy grown on Si(001) substrate.
- The β-$FeSi_2$(100) plane is bonded to the Si(001) plane with two Si dimers per unit cell.
- DFT band calculations suggest two dimensional metallic electronic states at the the β-$FeSi_2$/Si(001) interface.

Atomic and electronic structures of the β-$FeSi_2$/Si(001) interface

Keisuke Sagisaka[a,*], Kazutaka Mitsuishi[a]

[a] *Center for Basic Research on Materials, National Institute for Materials Science, 1-2-1 Sengen, Tsukuba, 305-0047, Ibaraki, Japan*

Abstract

The atomistic interface structure between β-$FeSi_2$ and Si substrate was investigated by cross-sectional scanning transmission electron microscopy and density functional theory calculations (DFT). A high quality single crystalline β-$FeSi_2$ film was epitaxialy grown on Si(001) substrate. We demonstrate that the β-$FeSi_2$(100) plane is bonded to the Si(001) plane with two Si dimers per unit cell. With such interface structure, DFT band calculations reveal that metallic electronic states are localized at the interface. This finding implies the presence of two dimensional electronic states at the interface of β-$FeSi_2$/Si(001), which may have potential applications in silicon-based electronic devices.

Keywords: Iron silicide, Interface structure, STEM, DFT, STM

1. Introduction

β-iron silicide (β-$FeSi_2$) is a promising semiconducting material for light-emitting diode (LED) applications integrated into silicon electronic devices. Since the light emitting property at wavelength of 1.5 μm, relevant to optical fiber communication, was reported [1], significant efforts have been devoted to realizing infrared LEDs using this silicon-based material.[2, 3, 4, 5, 6, 7, 8, 9, 10] For the fabrication of these devices, Si(001) or Si(111) substrate is typically employed to grow β-$FeSi_2$ for integration with silicon electronic devices. These substrates also serve as a beneficial source of silicon. It is

*Corresponding author

Email address: SAGISAKA.Keisuke@nims.go.jp (Keisuke Sagisaka)

critical to grow a continuous epitaxial β-$FeSi_2$ film due to its superior emission performance compared to β-$FeSi_2$ nano-particles buried in Si. [11, 12]

Si and β-$FeSi_2$ exhibit compatible lattice constants, facilitating the epitaxial growth of β-$FeSi_2$ on a Si wafer. β-$FeSi_2$ possesses an orthorhombic unit cell with dimensions of $\boldsymbol{a} = 0.986$ nm, $\boldsymbol{b} = 0.779$ nm, and $\boldsymbol{c} = 7.83$ nm. [13] When using a Si(001) substrate, which is prevalent in the electronic device industry, the (100) plane of β-$FeSi_2$ is grown with azimuthal orientations rotated by 45° relative to the substrate surface normal (Fig. 1). Despite the good crystallographic match between β-$FeSi_2$ and Si(001), small strains are anticipated along the b and c axis of β-$FeSi_2$, amounting to 1.4% and 2.0%, respectively. While β-$FeSi_2$ tends to form islands on the Si(001) substrate at high growth temperatures (at 700°C or above), [14] a flat and continuous epitaxial film can be achieved by employing a lower growth temperature ($\sim$470°C). [15, 16, 17] This thin film has been utilized as a template for the subsequent growth of thicker continuous films. [18, 19, 20]

The performance of β-$FeSi_2$ LEDs remains unsatisfactory for practical applications. One proposed reason for this is the low quantum efficiencies for electroluminescence, which is attributed to non-radiative recombination through defects at the β-$FeSi_2$/Si interface. [12] Additionally, the interface morphology may affect photoluminescence. [21] Furthermore, the thin epitaxial film of β-$FeSi_2$ directly grown on the Si(001) substrate at low temperature ($\sim$470°C) exhibits a intriguing feature of an undulating surface without steps. [16, 17] The mechanism of formation and stress relaxation of such a membrane are not well understood. Therefore, detailed knowledge of the atomistic interface structure between β-$FeSi_2$/Si(001) is essential for addressing these issues, as well as for controlling epitaxial growth and managing strains induced in the film. However, the interface structure between β-$FeSi_2$/Si(001) has not yet been identified.

In this paper, we elucidate the atomistic structure of the β-$FeSi_2$/Si(001) interface based on observations made using cross-sectional scanning transmission electron microscopy (STEM), supported by density functional theory (DFT) calculations. The detailed characterization of the interface structure promoted us to calculate its electronic structure. Consequently, we determined that the electronic property of the interface is metallic, characterized by two bands crossing the Fermi level. This finding suggests the realization of a two-dimensional (2D) electronic state at the interface of β-$FeSi_2$/Si(001).

2. Methods

2.1. Experiment

The preparation of the thin β-$FeSi_2$ was conducted in an ultrahigh vacuum (UHV) chamber with a base pressure of 5×10^{-9} Pa. A Si(001) substrate (n-type, resistivity: ~ 0.01 Ωcm) was flashed to 1100 °C for 10 seconds to obtain a clean surface after overnight degassing. A thin film of β-$FeSi_2$ was grown by depositing iron at a controlled deposition rate of 0.006 Å/s from a high-purity iron rod (99.995 %) onto the clean Si(001) surface substrate at room temperature, followed by annealing to 430 °C for 30 minutes. The crystallinity of the film surface was confirmed using scanning tunneling microscopy (STM) (Unisoku USM-1200). Following STM observation, the β-$FeSi_2$ surface was capped with amorphous silicon ($\sim$10 nm thick, deposition rate: $\sim$0.014 Å/s) in the UHV chamber to protect the film from an air exposure during transport. Subsequently, the sample was cut into a small piece and thinned by a focused ion beam. The β-$FeSi_2$/Si(100) interface was examined using STEM (JEOL JEM-ARM200F) operated at 200 kV.

2.2. Computation

The β-$FeSi_2$/Si(001) interface was modeled by a slab consisting of three unit layers of β-$FeSi_2$ and 21 Si atomic layers (Fig. S1 in the supplementary material). The top layer of β-$FeSi_2$ and the bottom layer of silicon were terminated with pseudo-hydrogen atoms (charge = 1.5) [22] and hydrogen atoms (charge = 1.0), respectively. Prior to STEM simulation and band calculations, structural optimizations of the slab were conducted by the VASP code [23, 24] with planewave basis sets (cutoff energy: 500 eV) and the Perdew-Burke-Ernzerhof exchange correlation [25] until forces were reduced to less than 0.01 eV/Å. A $8 \times 8 \times 1$ or $22 \times 22 \times 1$ Monkhorst-Pack k-point mesh sampling [26] was adopted for the structural optimizations or electronic calculations, respectively. STEM image simulations were conducted by the multislice method using the xHREM software (HREM Research Inc.), based on structure models obtained from the structural optimization of the slab model.

3. RESULTS AND DISCUSSION

Initially, the quality of a β-$FeSi_2$ film grown on a Si(001) substrate was confirmed by STM. The surface of the β-$FeSi_2$ film exhibits undulations along

the [100] and [010] crystallographic directions, forming interconnected patchy features with variations in the image contrast and dimension spanning several nanometers (Fig. 2). The height variation over the image is a root-mean square (RMS) of 0.11 nm. Notably, this surface of the β-$FeSi_2$ film does not exhibit stepped or polycrystalline characteristics, but rather forms a continuous surface. The surface is terminated with Si tetramers, which appear as a $p(2 \times 2)$ structure in the STM images, [16, 17] as shown in the inset of Fig. 2. This superstructure covers the surface continuously and uninterruptedly, even over regions that appear to have different heights in STM [Fig. S3 in the supplementary material]. These observations suggest that the β-$FeSi_2$ film cover the stepped Si substrate similarly to how a carpet covers stairs.

After the STM observation, the β-$FeSi_2$ film was capped by amorphous Si and its cross section was examined using STEM. In the low magnification image [Fig. 3(a)], the layer with the brightest contrast corresponds to the β-$FeSi_2$ film, which is situated between the Si substrate and Si capping layer. The STEM survey was conducted at multiple locations to confirm that the β-$FeSi_2$ film is a continuous single crystal. The film exhibits three different thicknesses: 1.0, 1.5 and 2.0 nm, which respectively correspond to 1, 1.5 and 2 unit layer of β-$FeSi_2$ along the [001] crystal orientation ($\boldsymbol{a} = 0.986$ nm).

At higher magnification, atomic arrangements in both the β-$FeSi_2$ film and the Si substrate are resolved [Fig. 3(b)]. This observation revealed that the relative configuration between β-$FeSi_2$ and Si substrate lattice remains constant across more than 30 lattice periods in all examined crystallographic orientations, including [110], [$\bar{1}$10], and [010] of Si [Fig. 3(b)]. These finding indicate that the commensurate epitaxial growth of the β-$FeSi_2$ is achieved on the Si(001) surface within this narrow thickness range. To enable this commensurate growth, the lattice mismatches should be compensated by elastic strains of 1.4% in the b axis and 2.0% in the c axis of β-$FeSi_2$. Such commensurate growth is typically observed in thin layers of semiconductor heteroepitaxy even in the presence of a lattice mismatch between the growth layer and substrate. [27]

The film thickness of the β-$FeSi_2$ appears to be regulated at the interface with the silicon substrate, while maintaining a flat surface. Figure 3(c) demonstrates the film thickness varies from one unit cell thick ($\boldsymbol{a}$) to 1.5 times that at the interface with the substrate. If a step forms on the topmost surface, its height should be a multiple of half the length of $\boldsymbol{a}$ ($\sim$0.5 nm). However, the STM image in Fig. 2 exhibits a RMS height variation of only 0.11 nm, which is not due to the presence of steps. The STM profile in

Fig. 2 shows smooth height changes across the surface. Although the STM image contrast reflects both the electronic and physical heights, it is currently unknown which effect predominates in the STM image. In either case, it should be ascribed to strain included within the β-$FeSi_2$ film. The surface height variation of 0.1 to 0.15 nm in the STM images (Fig. 2 and Fig. S3) closely matches the interplanar spacing of Si (0.136 nm) along the [001] direction. This suggests that the observed surface ripples are likely induced by the stepped structure of the substrate beneath the β-$FeSi_2$ membrane. We hypothesize that the patchy structure observed in the STM image results from alternating patches of single-crystal β-$FeSi_2$, each patch rotated by 90°, which together form a continuous film. The lattice constants of the β-$FeSi_2$ unit cell differ between along the b- and c-axes, but the unit cell contracts to twice the lattice constant of Si(001), making the crystal symmetry equivalent along the b- and c- axes, except for the Fe1, Si1 and Si4 layers, as labeled in Fig. 1. While minor rearrangement in the atomic positions is required within these layers, it is possible to connect adjacent patches rotated by 90° relative to each other without breaking crystal symmetry. When two patches of β-$FeSi_2$ oriented along b-axis and c-axis are connected, with two Si substrate lattices aligned and atomic positions adjusted to ensure a smooth transition between the respective layers, a net surface height variation of approximately 0.1 nm is expected. This variation, caused by the relative shift of one atomic layer in the crystal symmetry of Si substrate between the (110) and $(1\bar{1}0)$ planes, is consistent with the features observed in the STM images. Moreover, while the connection of rotated patches likely induces strain within the membrane, the overall stain should be minimized compared to a structure without patch rotations. However, this scenario remains hypothetical, and further investigations are necessary to confirm the structural characteristics of the thin β-$FeSi_2$ film grown on Si(001).

In contrast to our results, Takemoto *et al.* recently reported that β-$FeSi_2$ grown on a Si(001) substrate with a low anneal temperature (450 °C), similar to our sample in the present study, exhibited minimal strain (0% and -0.3% in the b and c axis, respectively), based on the results of X-ray diffraction analyses. [28] They also observed a lattice mismatch between β-$FeSi_2$ and Si(001) substrate occurring every 20 periods of the Si lattice, a phenomenon is not observed in our study. To explain this small strain in their study, they postulated the existence of an interface layer to accommodate a weak interaction between the β-$FeSi_2$ and Si(001) substrate. To address the atomistic structure at the interface, we conducted higher resolution STEM

observations.

The left panels in Fig. 4 show experimental STEM images of the β-$FeSi_2$/Si(001) interface at three distinct cross-sectional Si planes : (110), $(1\bar{1}0)$, and (100). Within the (110) and $(1\bar{1}0)$ planes, the appearance of β-$FeSi_2$ thin film, characterized by alternating vertical and horizontal ovals, is equivalent except the interface. In contrast, within the (100) plane, the atomic arrangement exhibits two discernible types cf contrast and a higher degree of packing compared to the other orientations. These observed features can be elucidated by considering the bulk structure of β-$FeSi_2$. Simulated STEM images, illustrated in the middle panel of Fig. 4, utilizing a slab model of β-$FeSi_2$/Si(001) (depicted in the right panel of Fig. 4), demonstrated a noteworthy agreement with the experimental counterparts in terms of both Fe and Si atom configuration and contrast. These observation results are the evidence for the growth of the β-$FeSi_2$ thin film. Note that the TEM image presented by Takemoto *et al.* [28] does not align with any of the aforementioned images of β-$FeSi_2$ in Fig. 4, but rather looks similar to the TEM image of γ-$FeSi_2$ reported by Nissen *et al.* [29]

A further discussion focuses on the interface structure. We have examined several different structural models for the layer denoted as Si0 in Fig. 4. The structural model provided in Fig. 4 yields the best match between experimental and simulated images and also provides the lowest energy among tested models. [30] The characteristic feature of this interface structure is that β-$FeSi_2$ is stacked on dimers of Si atoms (bond length = 2.51 Å) located in the Si0 layer. The detailed atom's coordinates at the interface can be found in Fig. S2 and Table S1 in the supplementary material.

Utilizing the interface model represented in Fig. 4, we calculated its electronic structure. The bands indicated by red dots displayed in Fig. 5 are predominantly localized over Fe atoms in the Fe1 interface layer. These bands originate from the 3d orbitals of the Fe atoms and the 2p orbitals of Si dimers (Fig. S7 in the supplementary material). The corresponding charge density maps are found in Fig. S5 in the supplementary material. These bands are dispersive within the plane parallel to the interface, with two of them crossing the Fermi energy. This observation yields an estimated carrier density of 1.46×10^{14} cm^{-2}. The plot of these bands around the Fermi level within the first Brillouin zone (BZ) reveals a 2D character (Fig. 6). Since these bands appear within the bulk band gaps of both β-$FeSi_2$ and Si, carrier transport is expected to occur along the interface. Based on the analysis of PDOS (Fig. S6 in the supplementary material), the states associated with

these bands decay to 46% in the Fe2 layer and further diminished to 6% in the Fe3 layer. Therefore, even with the presence of a faceted interface geometry, with a height of approximately half unit cell ($\sim$5 Å) as shown in Fig. 3(c), the metallic properties are expected to persist. On the other hand, the shapes of the bands in the first BZ near the Fermi energy vary considerably with energy. Consequently, fluctuations in the Fermi energy, due to doping conditions in the substrate or the β-$FeSi_2$ film and other factors, can significantly alter the transport properties. We also conducted spin-polarized calculation, resulting in spin-polarized bands for interface (Fig. S9 in the supplementary material). However, since energy gain due to spin-polarized calculation is only 33 meV, spin-polarized transport may be not achieved by thermal smearing at room temperature.

4. Conclusion

We unambiguously determined the atomistic interface structure of β-$FeSi_2$/Si(001) epitaxially grown on a Si(001) substrate based on cross-sectional STEM observations and DFT calculations. The (001) planes of β-$FeSi_2$ and Si bond to each other with two Si dimers per unit cell of β-$FeSi_2$. For the β-$FeSi_2$ thicknesses used in this study, commensurate epitaxial growth of β-$FeSi_2$ and defect-free interface were achieved. Additionally, surface undulations observed by STM indicate that the β-$FeSi_2$ thin film is strained. The formation mechanism of the carpet-like film remains an open question for future study. Furthermore, DFT band calculation revealed metallic electronic states at the interface, suggesting that the β-$FeSi_2$/Si(001) interface could be a new 2D material.

2D materials, such as graphene, MXenes, transitional metal dichalcogenide monolayers, generally refers to single-layer material, require a heterostructure to decouple from a substrate and environment, enabling the use of their intrinsic properties. Using an insulator such as hexagonal boron nitrite can protect their 2D properties both electronically and chemically. The 2D system realized at the β-$FeSi_2$/Si(001) interface is inherently protected by these materials. Experimental verification of the properties of this new material through transport measurement is necessary.

CRediT author statement

Keisuke Sagisaka: Conceptualization, Project administration, Investigation, Formal analysis, Visualization, Writing – Original draft, Writing –

Review and Editing. **Kazutaka Mitsuishi**: Investigation, Formal analysis, Writing – Review and Editing.

Declaration of competing interest

The authors declare that they have no known competing financial interests or personal relationships that could have appeared to influence the work reported in this paper.

Acknowledgements

We gratefully acknowledge Tomoko Kusawake for providing expert technical assistance with sample preparation. We also thank David Bowler and Jun Nara for their valuable discussions on DFT computational techniques. The work was supported by JSPS KAKENHI (Grant Nos. 17K04985 and 22K04860). Computational simulations were performed on the NIMS numerical simulator.

5. Data availability

The data that support the findings of this study are available from the corresponding authors upon reasonable request.

References

[1] D. Leong, M. Harry, K. J. Reeson, K. P. Homewood, A silicon/iron-disilicide light-emitting diode operating at a wavelength of 1.5 μm, Nature 387 (1997) 686.

[2] T. Suemasu, Y. Negishi, K. Takakura, F. Hasegawa, Room Temperature 1.6 μm Electroluminescence from a Si-Based Light Emitting Diode with β-$FeSi_2$ Active Region, J. J. Appl. Phys. 39 (10B) (2000) L1013.

[3] T. Suemasu, Y. Negishi, K. Takakura, F. Hasegawa, T. Chikyow, Influence of Si growth temperature for embedding β-$FeSi_2$ and resultant strain in β-$FeSi_2$ on light emission from p-Si/β-$FeSi_2$ particles/n-Si light-emitting diodes, Appl. Phys. Lett. 79 (12) (2001) 1804–1806.

[4] T. Suemasu, K. Takakura, C. Li, Y. Ozawa, Y. Kumagai, F. Hasegawa, Epitaxial growth of semiconducting β-$FeSi_2$ and its application to light-emitting diodes, Thin Solid Films 461 (1) (2004) 209–218.

[5] S. Chu, T. Hirohada, H. Kan, T. Hiruma, Electroluminescence and Response Characterization of β-$FeSi_2$-Based Light-Emitting Diodes, J. J. Appl. Phys. 43 (2A) (2004) L154.

[6] T. Sunohara, C. Li, Y. Ozawa, T. Suemasu, F. Hasegawa, Growth and Characterization of Si-Based Light-Emitting Diode with β-$FeSi_2$-Particles/Si Multilayered Active Region by Molecular Beam Epitaxy, J. J. Appl. Phys. 44 (6R) (2005) 3951.

[7] M. Takauji, C. Li, T. Suemasu, F. Hasegawa, Fabrication of p-Si/β-$FeSi_2$/n-Si Double-Heterostructure Light-Emitting Diode by Molecular Beam Epitaxy, J. J. Appl. Phys. 44 (4S) (2005) 2483.

[8] K. Akiyama, S. Kaneko, Y. Hirabayashi, H. Funakubo, Photoluminescence properties of Si/β-$FeSi_2$/Si double heterostructure, Thin Solid Films 508 (1) (2006) 380–384.

[9] C. Li, T. Suemasu, F. Hasegawa, Temperature dependence of electroluminescence from Si-based light emitting diodes with β-$FeSi_2$ particles active region, J. Lumin. 118 (2) (2006) 330–334.

[10] Y. Ugajin, M. Takauji, T. Suemasu, Annealing temperature dependence of EL properties of Si/β-$FeSi_2$/Si(111) double-heterostructures light-emitting diodes, Thin Solid Films 508 (1) (2006) 376–379.

[11] S. Chu, T. Hirohada, K. Nakajima, H. Kan, T. Hiruma, Room-Temperature 1.56 μm Electroluminescence of Highly Oriented β-$FeSi_2$/Si Single Heterojunction Prepared by Magnetron-Sputtering Deposition, J. J. Appl. Phys. 41 (11A) (2002) L1200. .

[12] D. Chi, Semiconducting beta-phase $FeSi_2$ for light emitting diode applications: Recent developments, challenges, and solutions, Thin Solid Films 537 (2013) 1–22.

[13] Y. Dusausoy, J. Protas, R. Wandji, B. Roques, Structure cristalline du disiliciure de fer, $FeSi_2\beta$, Acta Crystallogr. B 27 (6) (1971) 1209–1218.

[14] T. Suemasu, M. Tanaka, T. F. Hashimoto, Y. Kumagai, F. H. F. Hasegawa, Aggregation of Monocrystalline β-$FeSi_2$ by Annealing and by Si Overlayer Growth, J. J. Appl. Phys. 36 (9A) (1997) L1225.

[15] M. T. M. Tanaka, Y. K. Y. Kumagai, T. S. T. Suemasu, F. H. F. Hasegawa, Formation of β-$FeSi_2$ Layers on Si(001) Substrates, J. J. Appl. Phys. 36 (6R) (1997) 3620.

[16] O. Romanyuk, K. Hattori, M. Someta, H. Daimon, Surface structure and electronic states of epitaxial β-$FeSi_2$(100)/Si(001) thin films: Combined quantitative LEED, ab initio DFT, and STM study, Phys. Rev. B 90 (2014) 155305.

[17] K. Sagisaka, T. Kusawake, D. Bowler, S. Ohno, Emergence of metallic surface states and negative differential conductance in thin β-$FeSi_2$ films on Si(001), Journal of Physics: Condensed Matter 35 (13) (2023) 135001.

[18] N. Hiroi, T. Suemasu, K. Takakura, N. Seki, F. Hasegawa, Direct Growth of [100]-Oriented High-Quality β-$FeSi_2$ Films on Si(001) Substrates by Molecular Beam Epitaxy, J. J. Appl. Phys. 40 (10A) (2001) L1008.

[19] T. Sunohara, K. Kobayashi, T. Suemasu, Epitaxial growth and characterization of Si-based light-emitting Si/β-$FeSi_2$ film/Si double heterostructures on Si(001) substrates by molecular beam epitaxy, Thin Solid Films 508 (1) (2006) 371–375.

[20] S. Murase, T. Sunohara, T. Suemasu, Epitaxial growth and luminescence characterization of Si/β-$FeSi_2$/Si multilayered structures by molecular beam epitaxy, J. Cryst. Growth 301-302 (2007) 676–679.

[21] Y. Maeda, Y. Terai, M. Itakura, N. Kuwano, Photoluminescence properties of ion beam synthesized β-$FeSi_2$, Thin Solid Films 461 (1) (2004) 160–164.

[22] The results of the examination of the top surface termination using pseudo-hydrogen atoms with various charge quantities are provided in the supplementary material.

[23] G. Kresse, J. Hafner, Ab initio molecular dynamics for liquid metals, Phys. Rev. B 47 (1993) 558–561.

[24] G. Kresse, J. Furthmüller, Efficient iterative schemes for ab initio total-energy calculations using a plane-wave basis set, Phys. Rev. B 54 (1996) 11169–11186.

[25] J. P. Perdew, K. Burke, M. Ernzerhof, Generalized gradient approximation made simple, Phys. Rev. Lett. 77 (1996) 3865–3868.

[26] H. J. Monkhorst, J. D. Pack, Special points for brillouin-zone integrations, Phys. Rev. B 13 (1976) 5188–5192.

[27] J. M. Hartmann, A. Abbadie, S. Favier, Critical thickness for plastic relaxation of SiGe on Si(001) revisited, J. Appl. Phys. 110 (8) (2011) 083529.

[28] S. Takemoto, K. Hattori, M. Someta, A. N. Hattori, H. Tanaka, K. Kurushima, Y. D. H. Otsuka, Shape-fitting analyses of two-dimensional X-ray diffraction spots for strain-distribution evaluation in a β-$FeSi_2$ nanofilm, J. Appl. Cryst. 52 (2019) 732–744.

[29] H.-U. Nissen, E. Müller, H. R. Deller, H. Von Känel, TEM investigation of iron disilicide films on Si(001) grown by molecular beam epitaxy, Phys. Status Solidi A 150 (1) (1995) 395–406.

[30] Representative slab models tested in this work, along with their energetic stability, can be found in Fig. S1 in the supplementary material.

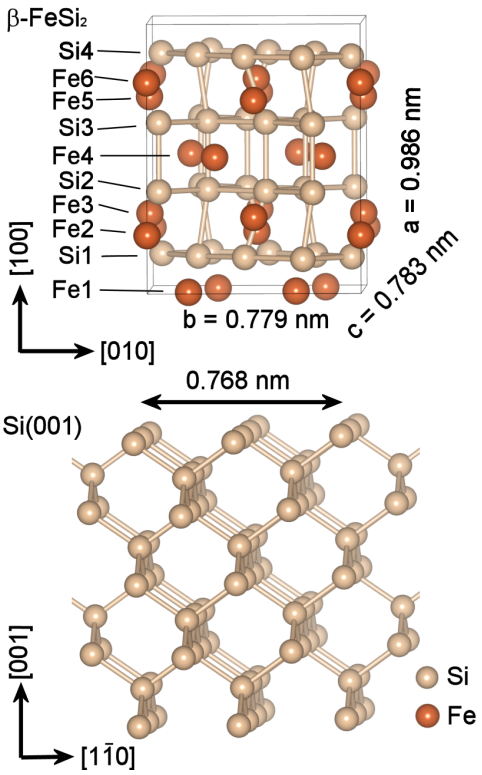


Figure 1: Stick-and-ball models for the unit cell of β-$FeSi_2$ and Si(001) substrate.

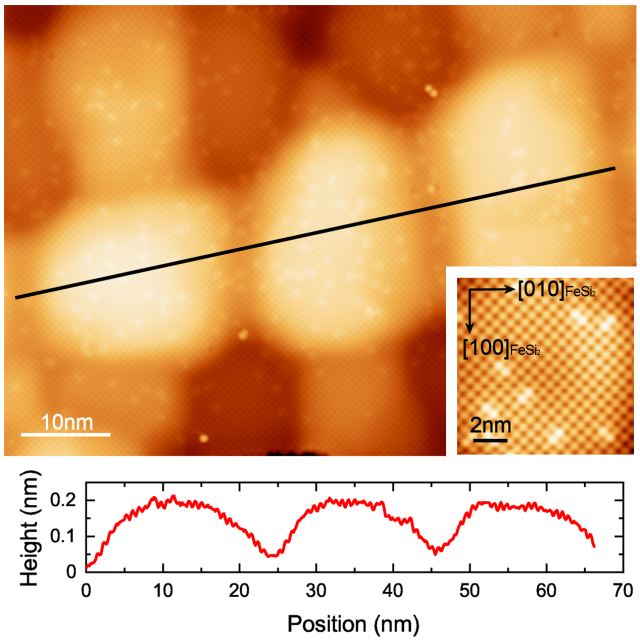


Figure 2: STM image of a β-$FeSi_2$ film grown on a Si(001) substrate. Imaging parameters: sample bias of -1.5 V, tunneling current of 3pA, and sample temperature of 4.3 K, The image dimensions are 70 $\times$ 50 nm^2, Inset: Sample bias of -1.0 V, tunneling current of 0.1 nA, and image dimensions of 10 $\times$ 10 nm^2, The bottom graph presents a cross-sectional profile along the indicated line in the STM image.

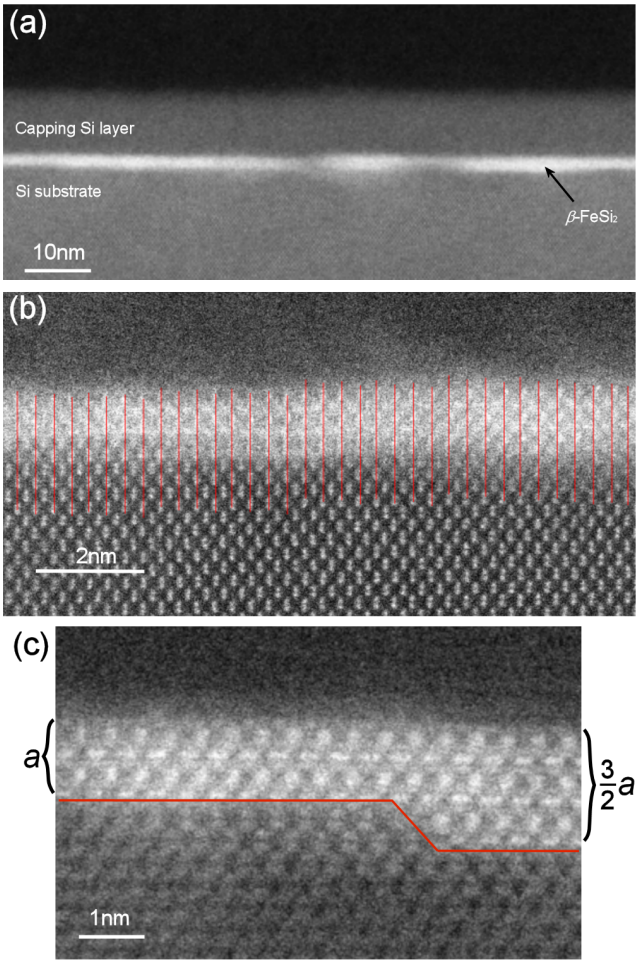


Figure 3: Cross-sectional STEM image of a β-$FeSi_2$ film grown on a Si(001) substrate. Horizontal image dimensions: (a) 65.7 nm, (b) 13.5 nm, (c) 6.5 nm. Red lines drawn in (b) and (c) serve as a visual guide to identify the commensurate configuration between the β-$FeSi_2$ and Si lattices and the interface, respectively.

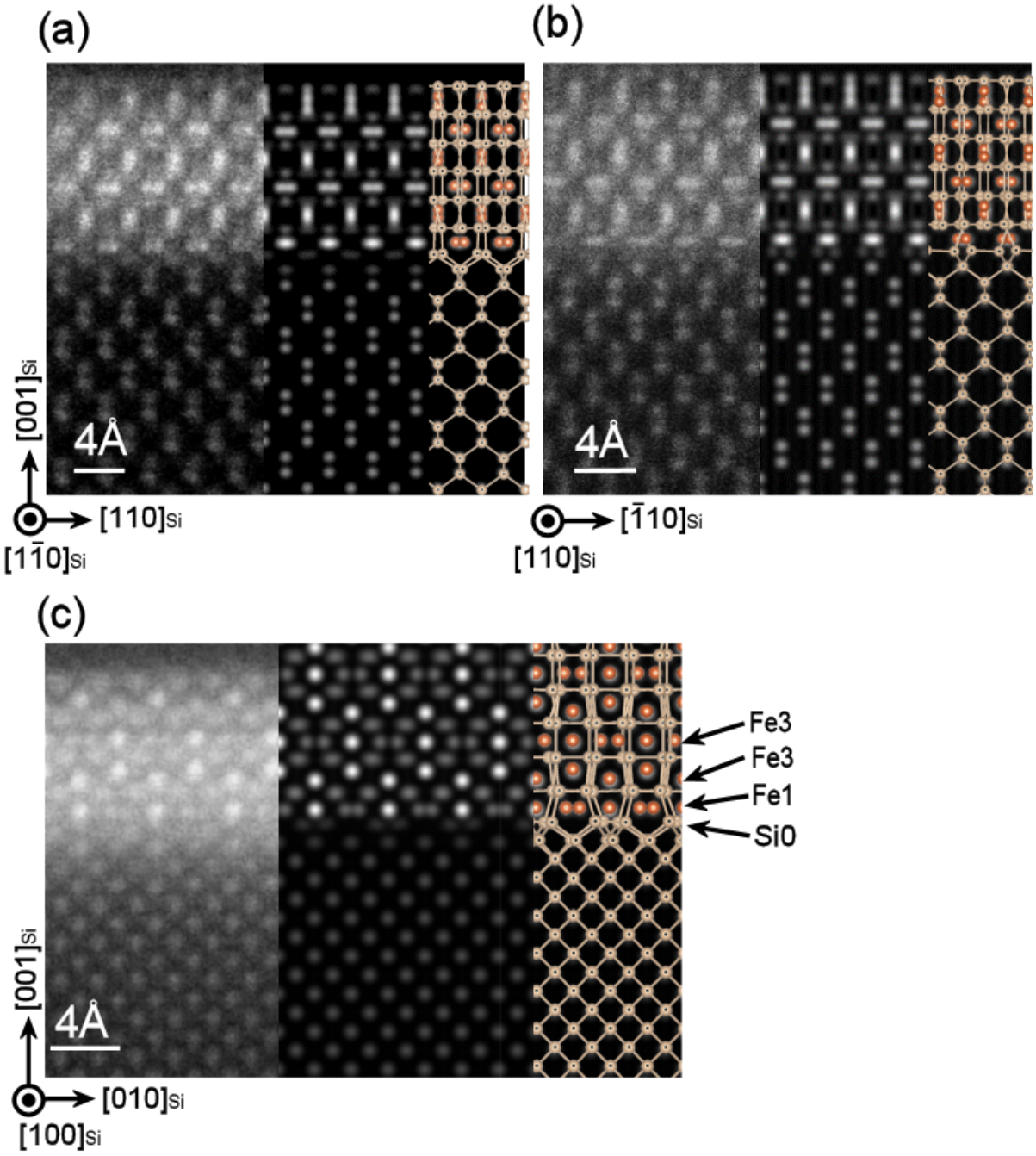


Figure 4: Experimental and simulated STEM images (Left and Middle) and structural model (Right) of the β-$FeSi_2$/Si(001) interface.

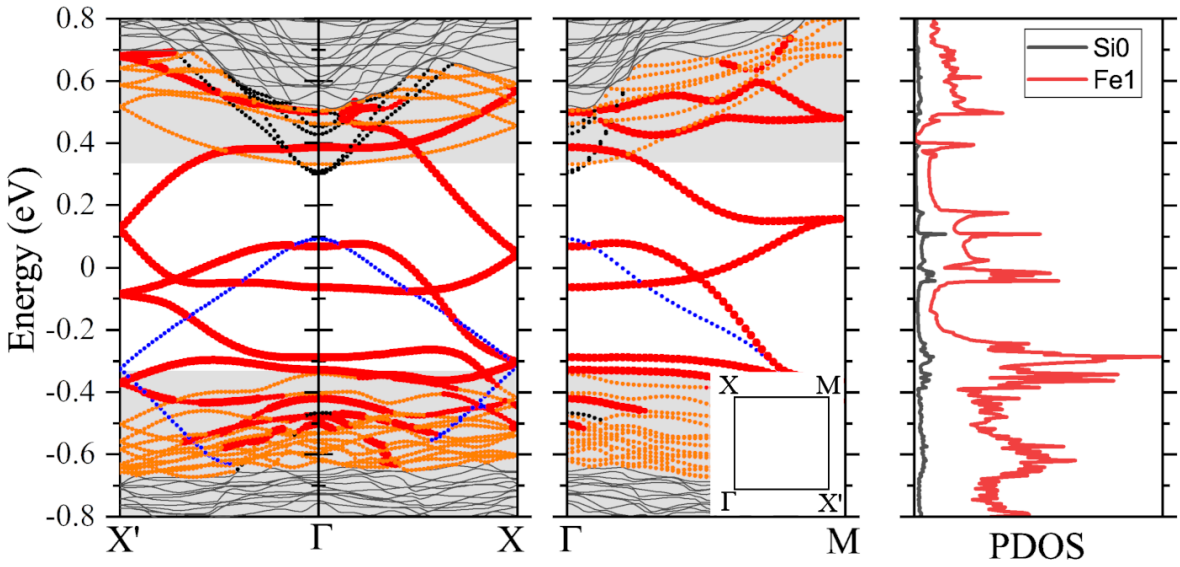


Figure 5: Band diagram projected onto the (001) plane and PDOS of the β-$FeSi_2$/Si(001) interface. The bands represented by red, orange, and black dots originate from the interface of β-$FeSi_2$/Si(001), bulk β-$FeSi_2$, and bulk Si, respectively. The bands represented by blue dots corresponds to the top most Si atoms of the slab, which are terminated with pseudo-H atoms. These assignments were performed by examining the charge density distribution of each eigenvalues within the slab. The bands depicted in black lines have not been examined for their origin. (Inset) The notation of the BZ is consistent with that used for the Si(001) surface.

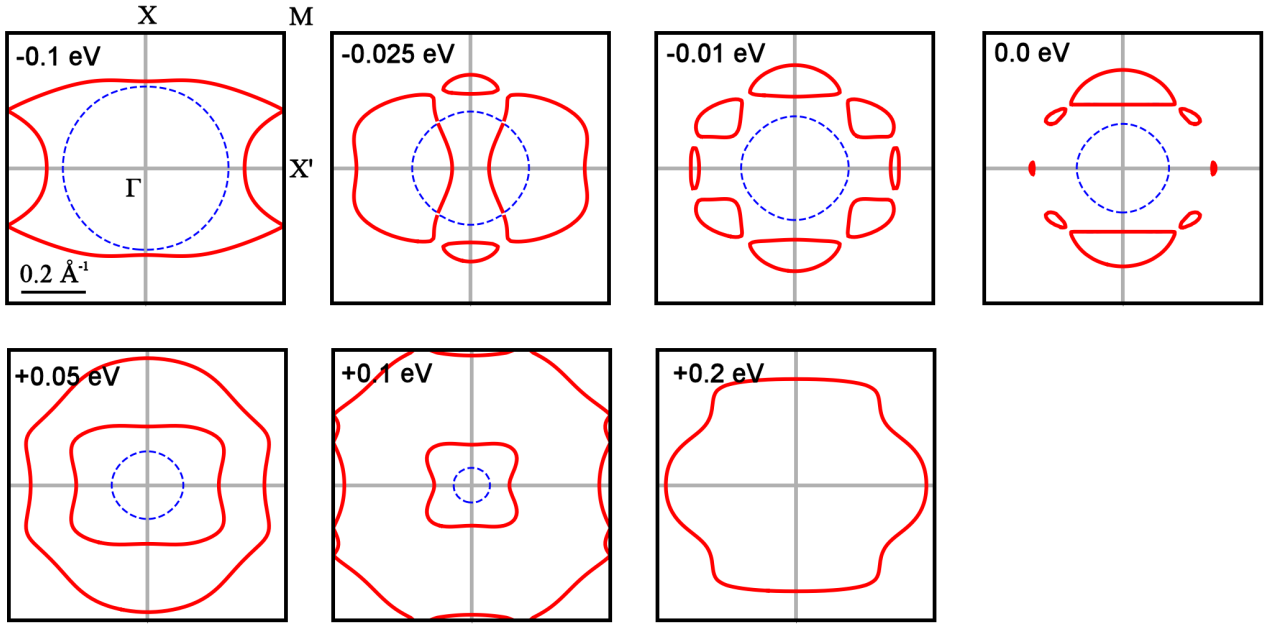


Figure 6: Contour maps for the β-$FeSi_2$/Si(001) interface bands within the first Brillouin zone at various energies around the Fermi level. The red lines represents the bands for the interface states, while the blue dashed circles denotes the bands for the topmost surface silicon atoms terminated by pseud-hydrogen atoms of the slab.